Transverse electrokinetic and microfluidic effects in micropatterned channels: Lubrication analysis for slab geometries

Armand Ajdari*
Laboratoire de Physico-Chimie Théorique, UMR CNRS 7083, ESPCI, 10 rue Vauquelin, F-75231 Paris Cedex 05, France
(Received 28 December 2000; revised manuscript received 27 August 2001; published 14 December 2001)

Off-diagonal (transverse) effects in micropatterned geometries are predicted and analyzed within the general frame of linear-response theory, relating applied pressure gradient and electric field to flow and electric current. These effects could contribute to the design of pumps, mixers, or flow detectors. Shape and charge-density modulations are proposed as a means to obtain sizeable transverse effects, as demonstrated by focusing on simple geometries and using the lubrication approximation.

DOI: 10.1103/PhysRevE.65.016301 PACS number(s): 47.65.+a, 83.60.Np, 85.90.+h

I. INTRODUCTION

The development of microfluidic devices and studies has prompted the quest for various strategies to achieve pumping in microgeometries [1–7]. Pressure-driven flows is the first obvious possibility, with the inconvenience of important Taylor dispersion due to the parabolic flow profiles [8]. Electro-osmosis has been proposed and developed as a way to generate almost perfect plug flows, thereby reducing dispersion in various devices, which results in limited dilution of samples, and processability for separation purposes [7]. This solution implies relatively high voltages applied between the ends of the channels.

In this paper, micropatterned channels are proposed as a way to generate a large class of effects using pressure gradients or electric fields. In particular, various off-diagonal effects may be obtained in which a cause along one direction leads to a measurable or useful effect in a perpendicular direction. These effects could be exploited for the realization of transverse pumps, mixers, flow detectors, etc. A proposed pattern is the periodic modulation of the shape of the channels, which may be improved by a combined modulation of the surface charge density. (in line with an earlier study that dealt with transverse electro-osmosis on such surfaces [9]). The aim is here to explore the ensemble of transverse effects achievable.

To reach this goal, the linear response regime is considered, which permits the use of a very general Onsager formalism, to relate fields (pressure and electric potential gradients) to currents (hydrodynamic flow and electric current). For the sake of clarity, we further restrain our analysis to a simple class of geometries, with the fluid confined between two parallel plates, homogeneously and periodically patterned (Fig. 1). Parallel walls may be present so as to form a channel.

In Sec. II, the geometry and the matrix representation for linear response are first given, then used to explain at the phenomenological level the off-diagonal effects for the case of passive walls (a few situations where electrodes are embedded in the walls are considered in Appendix A, and the corresponding wall-generated effects analyzed). In Sec. III, an explicit realization is described and estimates for the effects given. The calculations are performed using the lubrication approximation, and assuming weak surface potentials, which provides a convenient analytic handle. Results for sinusoidal modulations of the shape and charge densities are reported in Appendix B. A brief discussion closes the paper (Sec. IV), pointing out directions for future studies.

II. DIRECTIONAL COUPLING WITHIN LINEAR RESPONSE

A. Local linear response

We consider the Hele-Shaw quasiplanar geometry of Fig. 1, where the two sides of the slab bear periodic patterns of principal axes (x,y), and set the formalism relating two-dimensional (2D) fields to 2D currents (i.e., integrated over z) at the *local scale* (i.e., at a scale larger than the period of the pattern but smaller than the width of the channel). In the linear-response regime, the 2D currents (hydrodynamic flow $\mathbf{J}$ and electric current $\mathbf{J_{el}}$) are related to the 2D pressure gradient $\boldsymbol{\nabla} p$ and to the 2D electrostatic potential gradient $\boldsymbol{\nabla}\phi = -\mathbf{E}$, by a generalized conductance matrix [11]:

$$\begin{bmatrix} \mathbf{J} \\ \mathbf{J_{el}} \end{bmatrix} = \begin{bmatrix} \mathbf{K} & \mathbf{M} \\ \mathbf{M} & \mathbf{S} \end{bmatrix} \cdot \begin{bmatrix} -\boldsymbol{\nabla} p \\ -\boldsymbol{\nabla}\phi \end{bmatrix} \tag{1}$$

or equivalently by the generalized resistance matrix:

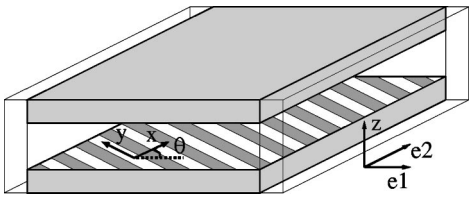

FIG. 1. Slab geometry considered in this paper: Two parallel walls bear on their inner faces periodic microfabricated patterns of principal axes x and y. The slab may be limited sideways by walls, the axis of the resulting channel e_2 at an angle θ with the y axis of the pattern. From Sec. III on, we focus on patterns periodic along x and invariant along y.

*Electronic address: armand@turner.pct.espci.fr

$$\begin{bmatrix} -\nabla p \\ -\nabla \phi \end{bmatrix} = \begin{bmatrix} \mathbf{k} & \mathbf{m} \\ \mathbf{m} & \mathbf{s} \end{bmatrix} \cdot \begin{bmatrix} \mathbf{J} \\ \mathbf{J_{el}} \end{bmatrix}, \tag{2}$$

where **K**, **M**, **S**, **k**, **m**, and **s** are 2×2 matrices, that are symmetric to satisfy Onsager relations [11].

The permeation matrix **K** describes the flow induced by pressure differences (the Darcy law in a porous medium). The conduction matrix **S** relates the electric current to the electric field (the medium's Ohm's law). The matrix **M** describes the electro-hydrodynamic coupling (so-called electrokinetic effects). In the first line of Eq. (1), it quantifies *electro-osmosis*, i.e., the hydrodynamic flow induced by the electric field. This effect stems from the presence of thin diffuse layers in the vicinity of charged walls where the fluid is non-neutral, and thus dragged by the local electric field. In the second line of Eq. (2), **M** measures the electric current induced by the presence of a net hydrodynamic flow. This is due to the convective transport of the above-mentioned charged layer that leads to an ionic current. The result is hydrodynamically generated electrostatic potential differences (''streaming potentials'') and electric currents (''streaming currents'').

All the above is standard in the 1D geometry of cylindrical capillaries, or for homogeneous and isotropic porous media, where *K*, *S*, and *M* are scalars. Here, we explore the phenomena occurring in the present 2D geometry with non-equivalent properties along the *x* and *y* axes, allowing for the existence of off-diagonal effects.

Indeed, the 2×2 matrices in Eqs. (1) and (2) are diagonal in the principal axes (*x*,*y*), but not in the basis (e_1,e_2) related to the overall channel geometry (see Fig. 1). To set notations, if one of them reads $\mathbf{F}=F_x\mathbf{xx}+F_y\mathbf{yy}$, its expression $\mathbf{F}=\Sigma_{1,2}F_{i,j}\mathbf{e}_i\mathbf{e}_j$ in the basis (e_1,e_2) is

$$\mathbf{F}=\begin{pmatrix} F_x\cos^2\theta+F_y\sin^2\theta & (F_x-F_y)\sin\theta\cos\theta \\ (F_x-F_y)\sin\theta\cos\theta & F_y\cos^2\theta+F_x\sin^2\theta \end{pmatrix}. \tag{3}$$

It is then obvious that, locally, nondiagonal or transverse effects (a cause along e_1 induces an effect along e_2 or the reverse) occur if some of the local transverse coefficients K_{12}, M_{12}, or S_{12} are nonzero. From the above geometric formula, this requires $K_x\neq K_y$, $M_x\neq M_y$, or $S_x\neq S_y$, i.e., that the anisotropy in the pattern of the plates has translated into different local susceptibilities along the two principal axes *x* and *y*.

We postpone to Sec. III a description of a way to achieve this asymmetry, and start with a generic description of the effects expected if local anisotropy is present. As written above, the local Eqs. (1) and (2) already describe the transverse electrokinetic couplings that would occur in open geometries with no boundaries: for example, an electric field along e_1 generates a flow along e_2 (*transverse electro-osmosis*), and a flow along e_1 a *transverse streaming potential* along e_2. To be more practical, we wish now to explore the expression of these couplings in the channel geometry of Figs. 1 and 2, where the walls perpendicular to e_1 impose constraints on the fields and currents.

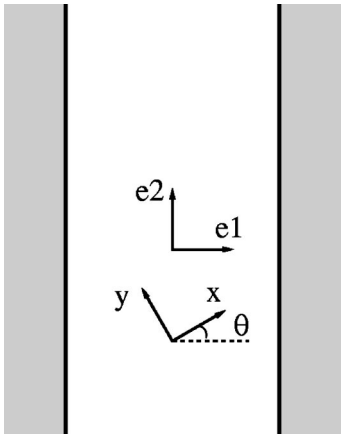

FIG. 2. Top view of the slab geometry of Fig. 1.

B. Channels with passive walls

Take a channel of length *L* along e_2 and width *d* along e_1, bounded by impermeable walls. We suppose here that no electric current may flow from one side to the other, so both currents in direction e_1 are on average zero: $J_1=0$ and $J_{el1}=0$. Potential differences between the two walls may however be measured using a set of electrodes connected by a high resistance in series with a voltmeter (Fig. 3). In this geometry, it is straightforward to quantify the effects generated by a forcing along the length of the channel (direction e_2).

1. Pressure-driven effects

Suppose a pressure drop Δp_2 is applied along the channel so that the average value of $\partial_2 p$ is $\Delta p_2/L$. We furthermore consider that there is no external electrical path connecting the two ends of the channel so that $J_{el2}=0$: any streaming current (along the walls) is compensated by a back current in the bulk.

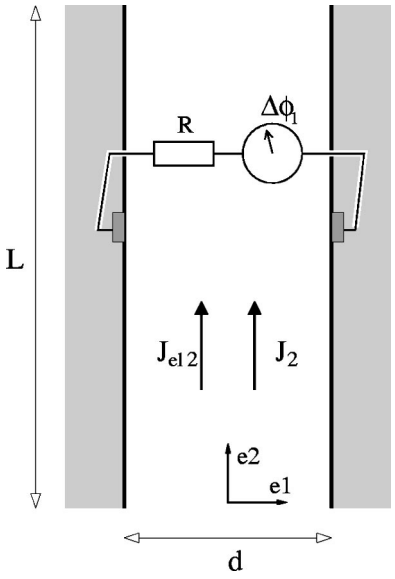

FIG. 3. Passive walls: Neither hydrodynamic flow nor electric current is possible along the e_1 axis. A potential difference $\Delta\phi_1$ may be measured using a high-input impedance voltmeter.

The application of the pressure drop Δp_2 then results in "classical" longitudinal effects along e_2: a total fluid flux $Q_2 = d\,J_2 = k_{22}^{-1}(d/L)(-\Delta p_2)$ (a Darcy law modified by electric effects), and a streaming potential $\Delta\phi_2 = (m_{22}/k_{22})\Delta p_2$.

More interestingly, transverse effects are also generated across the channel: a pressure difference Δp_1 and a potential drop $\Delta\phi_1$:

$$\Delta p_1 = (k_{12}/k_{22})(d/L)\Delta p_2, \tag{4}$$

$$\Delta\phi_1 = (m_{12}/k_{22})(d/L)\Delta p_2. \tag{5}$$

The *transverse pressure difference* Δp_1 exists if $k_{12} \neq 0$, in which case it indicates that recirculation is taking place in the e_1 direction: the pressure drop along e_2 entrains fluid in the e_1 direction, which, due to the presence of the walls, then has to recirculate. A certain amount of shearing and mixing is thus induced.

The *transverse streaming potential* $\Delta\phi_1$, proportional to the nondiagonal electrokinetic coefficient m_{12}, provides an electric measure of the hydrodynamic flow along e_2. Note that, this potential drop is intrinsically smaller than the streaming potential along the channel by a factor d/L due to the geometry of the system, times a factor m_{12}/m_{22} that need not be smaller than one (see, e.g., the end of Sec. III and Appendix B).

2. Electrically driven effects

Suppose now that a total electric current $I_2 = d\,J_{el2}$, or an average electric field E_2, is applied along a channel connected to large open reservoirs so that $\Delta p_2 = 0$. This yields standard effects along the channel, which are simply Ohm's law $J_{el2} = [k_{22}/(k_{22}s_{22} - m_{22}^2)]E_2$ and a longitudinal electro-osmotic solvent flux $Q_2 = d\,J_2 = -(m_{22}/k_{22})J_{el2} = -[m_{22}/(k_{22}s_{22} - m_{22}^2)]d\,E_2$.

In addition, transverse effects are generated,

$$\Delta p_1 = -\frac{m_{12}k_{22} - k_{12}m_{22}}{s_{22}k_{22} - m_{22}^2} d\,E_2, \tag{6}$$

$$\Delta\phi_1 = -\frac{s_{12}k_{22} - m_{12}m_{22}}{s_{22}k_{22} - m_{22}^2} d\,E_2. \tag{7}$$

Equation (6) indicates *transverse electro-osmosis*: the electric-field E_2 induces an electro-osmotic flow along e_1 (if $m_{12} \neq 0$), which due to the presence of the walls, leads to a pressure difference Δp_1 that drives recirculation of the fluid along e_1. Again, this induces shear and favors mixing. This effect is due both to the nondiagonal permeation (k_{12}) and to transverse electro-osmosis per se (m_{12}).

Equation (7) describes an "electrokinetic Hall effect": an electric field applied along e_2 results in an electrostatic potential difference along e_1, due to both the anisotropic conductivity (s_{12}) and the transverse streaming current (m_{12}).

C. Comments

Many other geometries may actually be envisaged, corresponding to various imposed boundary conditions for fluxes or potentials. In Appendix A, we consider situations where electrodes are embedded in the walls, which permits, for example, the generation of flow along the channel from transverse potential differences between the walls. Let us stress here a few general points.

Evaluation of the effect is easy only if the geometry (imposed boundary conditions) permits homogeneous solutions for the gradients and currents. Otherwise, one has to solve the 2D conservation equations for the currents.

This obviously would also be the case with heterogeneous patterns on the plates. We will return to this in the discussion section.

A more serious (less obvious) problem has to do with electrodes: the specificities of electrochemistry at their surface may require a description in terms of the fluxes of the various ions rather than the simple description in terms of an electric current of Appendix A, in addition to the many experimental problems involved (surface corrosion, generation of gas bubbles, etc.).

In the channel geometries considered here, modifying or controlling the electrical connection between the walls affects the longitudinal coefficients K_{22}, M_{22}, S_{22} (if off-diagonal coefficients are nonzero).

Clearly, several coefficients describe the various couplings allowed by symmetry in this linear theory. To give quantitative estimates for these coefficients and thus for the corresponding effects one has to deal with notoriously difficult (even at low Reynolds number) electro-hydrodynamic calculations. However, a useful guide may be developed using the lubrication approximation, as shown in the next section.

III. SPECIFIC CALCULATIONS WITHIN LUBRICATION APPROXIMATION

A. Geometry and approximations

In this section, modulating the shape and the charge density on the plates is proposed as an efficient patterning to obtain transverse effects. Explicit calculations of the matrix coefficients introduced in Sec. II A are performed, which provide an estimate of the off-diagonal effects listed in Sec. II B. For the analysis to remain simple, I focus on the specific case where the charge and/or surface pattern is periodic along the direction x and invariant along the perpendicular direction y. To set notations, the channel has a local thickness $h(x) = h_0 + \delta h(x)$, and modulated charge densities $\sigma_1(x)$ on the bottom plate and $\sigma_2(x)$ on the top one (Fig. 4). Further, the following assumptions are made:

(i) the modulation wavelength is larger than the gap so that lubrication approximation holds [10],

(ii) the ionic strength is high enough for the typical gap thickness h_0 to be much larger than the Debye length $\lambda_D = \kappa^{-1}$,

(iii) the surface potentials (or charge densities) are weak enough for the double layers to be well described by the

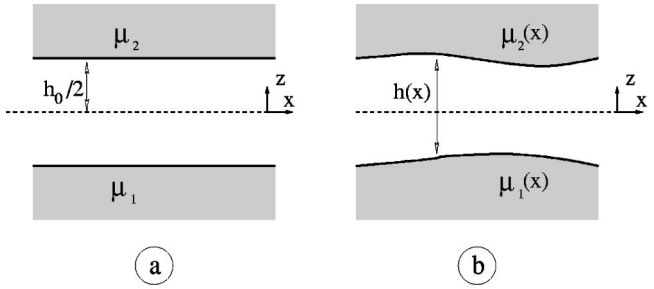

FIG. 4. Geometry considered in Sec. IV: (a) case of a uniform flat system, (b) the slip parameters describing electrokinetic effects and the thickness vary along x only.

Debye-Hückel theory. All effects are calculated to first order in these surface charge densities, so that terms proportional to products of σ_i are neglected altogether. This restriction comes in addition to (and is distinct from) the fact that we focus on the linear response of fluxes to applied fields.

Although these assumptions limit the quantitative precision of the results, they permit analytic calculations and thus a clear discussion of important qualitative features at a reasonably simple level, as well as estimates for the orders of magnitude of the effects.

To provide a clearer illustration, the following set of numerical values for the local parameters is used: water viscosity $\eta=10^{-3}$ Pa s, a 1:1 electrolyte at salt concentration 10^{-3} mol/l so that the Debye length is $\lambda_D\simeq 10^{-8}$ m and the conductivity $\gamma_{el}\simeq 10^{-2}$ m^2/V/s, and a charge density such that "electro-osmotic mobilities" are of order $\mu\simeq 2\times 10^{-8}$ m^2/V/s. This last assumption corresponds to surface electrostatic potentials of order k_BT at the limit of strict validity of the Debye-Hückel approximation. Whenever needed, the channel geometry will be described by a gap of $h_0=10$ μm, a width $d=200$ μm, and a length $L=2$ cm.

B. Flat and uniform surfaces

To get a physical insight, it is useful to start with the simple geometry of uniform flat surfaces [Fig. 4(a)]: $h(x)=h_0$, σ_1 and σ_2 constant. The computation of electrokinetic effects is then simple (given (ii) and (iii) [12]), and may be found in textbooks (e.g., [11]).

Electro-osmosis. If an electric field E is present in the channel, it will exert a drag on the thin charged Debye layer in the vicinity of the surfaces. The actual no-slip boundary condition for the solvent flow on the real surface of the plates may then be replaced by an electro-osmotic slip velocity $v_i=-\mu_i E$ on plate i, where $\mu_i=\sigma_i\lambda_D/\eta$, and η is the viscosity of water. This leads to a simple flow profile $v_{EO}(z)=-\mu_1 E(1-2z/h_0)-\mu_2 E(1+2z/h_0)$ and a net electro-osmotic flow through the channel $J_{EO}=-(\mu_1+\mu_2)h_0E/2$.

Poiseuille flow. In addition, there is naturally the pressure driven flow $v_{Poise.}=(z^2-h_0^2/4)\partial_x p/2\eta$ which gives a current $J_{Poise.}=-h_0^3\partial_x p/12\eta$.

Flow-induced current. This pressure-driven flow induces transport of the charged fluid of the Debye layers. If the local shear rate in the vicinity of the ith plate is $\dot\gamma$, the induced current is (per unit length in the y direction) $J_{eli}=-\sigma_i\lambda_D\dot\gamma=-\eta\mu_i\dot\gamma$. Given that $\dot\gamma=-h_0\partial_x p/2\eta$, this leads to a total current $J_{\mathrm{el}Flow\text{-}ind.}=(\mu_1+\mu_2)h_0\partial_x p/2$.

Ohm's law. Of course, the flow-induced current is often a minor correction to the main conduction current described by Ohm's law $J_{\mathrm{el}Ohm}=\gamma_{el}h_0E$.

Gathering all contributions, we are thus led to a scalar (in this isotropic case) version of Eq. (1),

$$J=\frac{h_0^3}{12\eta}(-\nabla p)-h_0\frac{\mu_1+\mu_2}{2}(-\nabla\phi), \tag{8}$$

$$J_{el}=-h_0\frac{\mu_1+\mu_2}{2}(-\nabla p)+\gamma_{el}h_0(-\nabla\phi). \tag{9}$$

The symmetry of the Onsager matrix is here clear.

Note that in principle, electro-osmotic flows also induce convective transport of the charged regions, which contributes an additional term of order $\sigma\mu E$ to the electric current J_{el}. However, this effect is proportional to $\sigma_i\sigma_j$ and neglected here given (iii). This is valid if $h_0\gg(\eta\mu^2/\gamma_{el}\lambda_D)$, a criterion fully satisfied by the numerical values proposed above for which it reads $h_0\gg 4$ nm.

C. Fields and currents along the modulation direction x

Returning to a channel periodically modulated along x, I consider first the case where the fluxes and gradients are applied along this axis. In this geometry, the currents J_x and $J_{\mathrm{el}x}$ are constants, whereas the local values of the pressure gradient $\partial_x p(x)$ and electric field $E_x(x)$ vary (although slowly enough in the lubrication approximation to consider them independent of z).

In the lubrication picture we can transcribe the results of the previous section

$$J_x=\frac{h^3(x)}{12\eta}(-\partial_x p(x))-h(x)\frac{\mu_1+\mu_2}{2}(x)E_x(x), \tag{10}$$

$$J_{\mathrm{el}x}=-h(x)\frac{\mu_1+\mu_2}{2}(x)(-\partial_x p(x))+\gamma_{el}h(x)E_x(x). \tag{11}$$

Then, neglecting along (iii) terms proportional to the product of σ_is (or μ_is), and performing integrals along x over a period of the modulation, gives

$$\begin{pmatrix}\langle-\partial_x p\rangle\\ \langle-\partial_x\phi\rangle\end{pmatrix}=\frac{12\eta}{\gamma_{el}}\begin{pmatrix}\gamma_{el}\left\langle\frac{1}{h^3}\right\rangle & \left\langle\frac{\mu_1+\mu_2}{2h^3}\right\rangle\\ \left\langle\frac{\mu_1+\mu_2}{2h^3}\right\rangle & \frac{1}{12\eta}\left\langle\frac{1}{h}\right\rangle\end{pmatrix}\begin{pmatrix}J_x\\ J_{\mathrm{el}x}\end{pmatrix}, \tag{12}$$

where $\langle f\rangle$ is the average of the function $f(x)$ over a period. With the same approximations, inversion yields:

$$\begin{pmatrix} J_x \\ J_{elx} \end{pmatrix} = \Delta_x \begin{pmatrix} \frac{1}{12\eta}\left\langle \frac{1}{h} \right\rangle & -\left\langle \frac{\mu_1+\mu_2}{2h^3} \right\rangle \\ -\left\langle \frac{\mu_1+\mu_2}{2h^3} \right\rangle & \gamma_{el}\left\langle \frac{1}{h^3} \right\rangle \end{pmatrix} \begin{pmatrix} \langle -\partial_x p \rangle \\ \langle -\partial_x \phi \rangle \end{pmatrix} \tag{13}$$

with $\Delta_x^{-1} = \langle 1/h^3 \rangle \langle 1/h \rangle$.

Note that approximation (iii) amounts here to $h^2 \gg 12\eta\mu^2/\gamma_{el}$, or $h \gg 20$ nm with the above numerical values, again easily verified for micron-sized gaps h_0.

D. Fields and currents along the perpendicular direction *y*

I now take fields and flows along the perpendicular direction *y*. In an infinite geometry, the electric-field E_y and the pressure gradient $\partial_y p$ are independent of *x*, whereas the currents are modulated along this direction:

$$J_y(x) = \frac{h^3(x)}{12\eta}(-\partial_y p) - h(x)\frac{\mu_1+\mu_2}{2}(x)E_y, \tag{14}$$

$$J_{ely}(x) = -h(x)\frac{\mu_1+\mu_2}{2}(x)[-\partial_y p(x)] + \gamma_{el}h(x)E_y. \tag{15}$$

Averaging over a period along *x* here gives

$$\begin{pmatrix} \langle J_y \rangle \\ \langle J_{ely} \rangle \end{pmatrix} = \begin{pmatrix} \frac{1}{12\eta}\langle h^3 \rangle & -\left\langle \frac{\mu_1+\mu_2}{2}h \right\rangle \\ -\left\langle \frac{\mu_1+\mu_2}{2}h \right\rangle & \gamma_{el}\langle h \rangle \end{pmatrix} \begin{pmatrix} -\partial_y p \\ -\partial_y \phi \end{pmatrix} \tag{16}$$

or upon inversion

$$\begin{pmatrix} -\partial_y p \\ -\partial_y \phi \end{pmatrix} = \Delta_y^{-1}\frac{12\eta}{\gamma_{el}} \begin{pmatrix} \gamma_{el}\langle h \rangle & \left\langle \frac{\mu_1+\mu_2}{2}h \right\rangle \\ \left\langle \frac{\mu_1+\mu_2}{2}h \right\rangle & \frac{1}{12\eta}\langle h^3 \rangle \end{pmatrix} \times \begin{pmatrix} \langle J_y \rangle \\ \langle J_{ely} \rangle \end{pmatrix} \tag{17}$$

with $\Delta_y^{-1} = \langle h^3 \rangle^{-1} \langle h \rangle^{-1}$.

E. Summary for arbitrary modulations

We may now write down the local coefficients of the response matrix to make the anisotropy in (x,y) explicit. The coefficient of the conductivity matrices (Sec. II) giving fluxes as functions of gradients are

$$K_x = \frac{1}{12\eta}\langle 1/h^3 \rangle^{-1}, \quad K_y = \frac{1}{12\eta}\langle h^3 \rangle, \tag{18}$$

$$S_x = \gamma_{el}\langle 1/h \rangle^{-1}, \quad S_y = \gamma_{el}\langle h \rangle, \tag{19}$$

$$M_x = -\frac{\left\langle \frac{\mu_1+\mu_2}{2h^3} \right\rangle}{\left\langle \frac{1}{h^3} \right\rangle \left\langle \frac{1}{h^1} \right\rangle}; \quad M_y = -\left\langle \frac{\mu_1+\mu_2}{2}h \right\rangle. \tag{20}$$

The anisotropy appears in a similar form in the "resistance matrix"

$$k_x = 12\eta\langle 1/h^3 \rangle; \quad k_y = 12\eta\langle h^3 \rangle^{-1}, \tag{21}$$

$$s_x = \frac{1}{\gamma_{el}}\langle 1/h \rangle; \quad s_y = \frac{1}{\gamma_{el}}\langle h \rangle^{-1}, \tag{22}$$

$$m_x = \frac{6\eta}{\gamma_{el}}\left\langle \frac{\mu_1+\mu_2}{h^3} \right\rangle; \quad m_y = \frac{6\eta}{\gamma_{el}}\frac{\langle (\mu_1+\mu_2)h \rangle}{\langle h \rangle \langle h^3 \rangle}. \tag{23}$$

The coefficients describing off-diagonal effects (Sec. II) are then obtained from these matrices expressed in the (e_1,e_2) frame [using Eq. (3)].

F. Discussion

To investigate semiquantitatively the consequences of the formulas derived above, a simple and practically relevant example is sinusoidal modulations of the shape and charge density [Fig. 5(a)],

$$h(x) = h_0(1 + \alpha\cos(qx)), \tag{24}$$

$$\mu_1 + \mu_2 = 2(\mu_0 + \delta\mu\cos(qx + \Theta)). \tag{25}$$

Analytical results take a simple form in the limit of weak modulation amplitudes for the shape, which allows us to calculate the result through an expansion in α.

This calculation is performed in Appendix B where this yields estimates for the ratios of nondiagonal to diagonal coefficients of the conductance and resistance matrix (e.g., m_{12}/m_{22}), which are one of the main ingredients that determines the amplitude of the transverse effects described in Sec. II B and Appendix A.

From this (see, in particular, the end of Appendix B), and from direct inspection of the formulas of the subsection above (Sec. III E), a few important points may be derived.

(i) A simple modulation of the charge pattern is not sufficient to induce off-diagonal effects. This is the consequence of the linear description in terms of the surface charge densities and of the $+/-$ symmetry (see, e.g., [9] for a discussion of this).

(ii) A modulation of the shape at homogeneous charge density is enough to produce off-diagonal effects for all phenomenologies (permeation $k_{12} \neq 0$, electro-osmosis and streaming potential/current $m_{12} \neq 0$, conductance $s_{12} \neq 0$). However, for a weak modulation $\delta h(x)$ around a mean h_0, the coupling coefficients will be proportional to $(\delta h/h_0)^2$.

(iii) A correlated coupling of the charge pattern and of the shape leads to stronger $O(\delta h/h_0)$ amplitudes for the off-diagonal electro-hydrodynamic couplings m_{12} and M_{12}. These off-diagonal couplings are proportional to $\delta\mu$, and

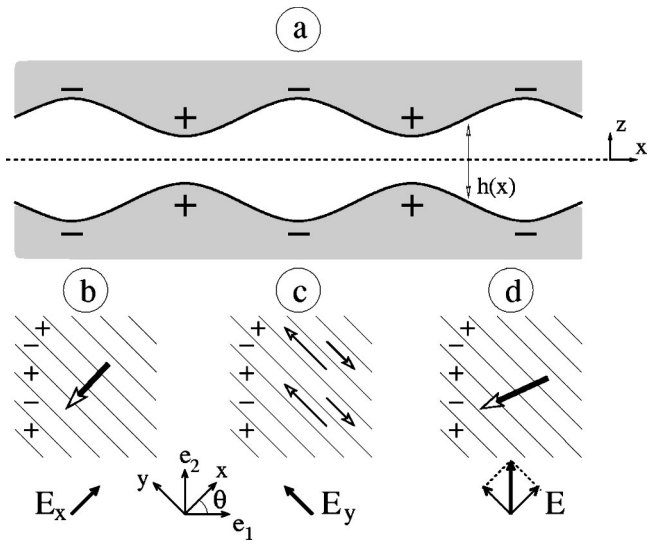

FIG. 5. Generation of off-diagonal effects (here electro-osmosis) from a sinusoidal modulation of shape and charge densities. The case depicted here (a) corresponds to $\alpha>0$, $\delta\mu>0$, $\Theta=\pi/2$, and a zero average charge density $\mu_0=0$. A schematic top view is then used in (b), (c), and (d), with $\theta=\pi/4$. (b) The field E_x generates a flow along x resulting from the opposite action of the narrow positively charged sections (tending to slip the fluid backwards along x) and of the wider negatively charged sections (which induce a slip in the positive direction). The thin sections dominate because of their stronger hydrodynamic resistance so the net flow is opposite to the applied field. (c) A field E_y applied along y induces a stratified flow with thin and wide sections again pushing in opposite directions. As the field is uniform, the slip velocities in the two directions are of similar amplitudes. Thus, the net flow is dominated by the wider sections, and points in the direction of the applied field. (d) Thanks to the linearity of the problem, the net flow created by a field E applied along e_2 is obtained by superimposing those obtained in (b) and (c), resulting here in a dominant transverse component.

may dominate the longitudinal ones if $\delta\mu/\mu_0 \gg 1$. This synergy between shape and charge modulation stems from the shape-induced symmetry breaking between plus and minus charges, and is described at length in [9] for the specific case of electro-osmosis. A schematic description is given in Fig. 5.

(iv) Extrapolation of these results to the case $\alpha\to 1$ (which does not necessarily contradict the lubrication approximation, see Appendix B), semiqualitatively suggests that the off-diagonal coefficients may all be of the same order than the diagonal ones. Favorable ingredients are a marked shape modulation ($\delta h/h\sim 1$), and a large charge modulation ($\delta\mu/\mu_0\sim 1$).

Then, in most cases, these ratios of nondiagonal to diagonal matrix coefficients that describe *local* couplings have to be multiplied by the geometrical factor d/L, to get the overall estimate of the *macroscopic* transverse effect. For example, pressure along a channel with passive walls induces across the channel width a transverse streaming potential that is smaller than the longitudinal one by a factor $(m_{12}/m_{22})(d/L)$. For a channel with a marked charge modulation around a weak average $\delta\mu/\mu_0\sim 10$ (acknowledgedly, a very favorable situation), $\alpha\sim 0.5$, one may get the first factor to be of order five so that for a channel of width $d=200$ μm and length $L=2$ cm, one obtains $\Delta\phi_1/\Delta\phi_2\sim 1/20$.

Let us end with rough estimates for the transverse effects described formally in Sec. II, using the numerical example proposed in Sec. III A, and assuming efficient transverse couplings in the limit $\alpha\to 1$. Using the values for local parameters of Sec. III A, the local matrix coefficients are in SI units $k_{ij}\simeq 10^{13}$, $m_{ij}\simeq 2\ 10^7$, and $s_{ij}\simeq 10^7$. We consider again a channel of length $L=2$ cm, width $d=200$ μm and typical gap $h_0=10$ μm.

(i) An applied pressure Δp_2 of order 1 atm generates (Sec. II B 1) flow velocities of order $v_2\sim 5$ cm/s, a longitudinal streaming potential $\Delta\phi_2\sim 0.2$ V, a *transverse streaming potential* $\Delta\phi_1\sim 2$ mV, and a *transverse pressure* $\Delta p_1\sim 1000$ Pa that induces transverse recirculations and mixing at velocities comparable to v_2.

(ii) An applied electric field of $E_2=500$ V/cm (a current $I_2\sim 10^{-6}$ A) generates longitudinal velocities of order $v_2\sim 1$ mm/s, as well as (Sec. II B 2) a transverse pressure of $\Delta p_1\sim 20$ Pa, and a *transverse potential* of order $\Delta\phi_1\sim 10$ V resulting mostly from the anisotropy of the Ohm's law in this geometry. Transverse recirculation and mixing also occurs in this electrically driven situation, again with transverse velocities comparable to v_2.

IV. CONCLUSION

We have shown that various off-diagonal effects may be generated using micropatterned geometries allowing for various functionalities: transverse pumping, mixing, flow detection, etc. The corresponding couplings may locally be of the same order as the usual (diagonal) electrokinetic coefficients (sometimes larger). Their actual global value depends on the geometry of the given device (through geometrical ratios such as, e.g., L/d). A detailed analysis for simple geometries of the flow pattern [variations in the third (z) direction] and thus of the mixing capabilities will be published elsewhere [15]. Obviously, more complex and realistic geometries (e.g., square-shaped grooves) are expected to lead to similar results, although their detailed performance may be assessed only numerically.

Realization of charge-patterned surfaces at the ten-micron scale has already been experimentally explored in simple geometries, for both soft elastomer systems [13], and more rigid plastic systems [14]. Its combination with shape modulations is clearly within the range of current microfabrication technologies [2,13,14], and is the topic of ongoing studies.

Naturally, more efficient devices for pumping, mixing, or flow detection should be realizable by playing with a larger class of patterns, including, in particular, inhomogeneous ones. A simple example is schematized in Fig. 6 where a vortex may be created by application of an electric field. Additional features or control can result from the increase of the third dimension: dealing with thicker fluid layers allows us, for example, to produce rolls with axes parallel to the surface [9,13]. Eventually, let us stress that although the focus of the present paper is on steady-state effects obtained with dc fields, interesting effects are also expected using ac fields and arrays of microelectrodes [3,4,16,17]. This great

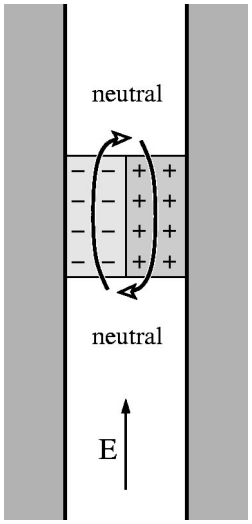

FIG. 6. A simple heterogeneous geometry to create a vortex (top view). No shape modulation, and a simple charge pattern: a positively charged zone aside a a negatively charged one (ideally both plates are patterned in the same way, i.e., floor and ceiling). The rest of the channel is neutral. The electro-osmotic slip generated by an electric field along the channel leads to a recirculation vortex as shown.

diversity of geometries imposes a hand-in-hand development of theoretical proposals and experimental realizations that we wish to pursue in the coming years.

ACKNOWLEDGMENTS

This work owes much to a continuous interaction with Abe Stroock, and I thank him for his permanent support, for many useful suggestions, and for a careful reading of the manuscript. Related discussions with Y. Chen, L. Locascio, D. Long, A. Pépin, and P. Tabeling are gratefully acknowledged.

APPENDIX A: WALLS SHORT CIRCUITED BY CONNECTED ELECTRODES

We again consider the geometry of Sec. III, but with the walls perpendicular to e_1 now covered by connected electrodes, so as to short circuit any electrostatic potential difference between the two walls.

Our picture here is very simplistic as we do not want to enter the detail of electrochemical reactions. Let us only make the following distinction (Fig. 7). First, in case (a), we will consider that these walls actually consist of a series of electrode pairs not connected between them, so that although the potential drop is on average zero in the e_1 direction, potential differences may nevertheless exist along the e_2 direction. In the second simplistic case (b), the walls are coated with continuous electrodes in which currents may circulate also along the e_2 direction so that the electrostatic potential is essentially constant $\Delta\phi_1=\Delta\phi_2=0$.

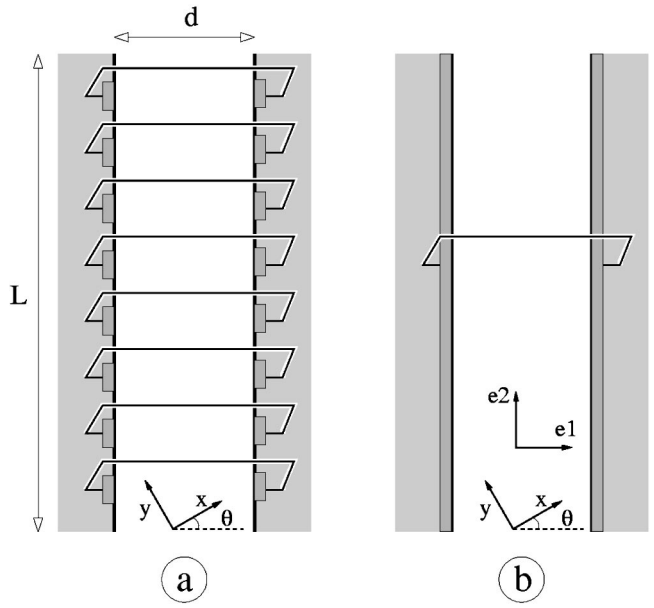

FIG. 7. (a) Connected electrodes; (b) the continuous electrodes short-circuit potential differences along the channel.

1. Series of connected electrodes

Pressure driven flow. In this geometry [Fig. 7(a)] ($J_{el2}=0$, $J_1=0$, $\Delta\phi_1=0$), an applied pressure difference along the channel $\Delta p_2\neq 0$ results in a streaming potential $\Delta\phi_2$ that differs from the one obtained with passive walls

$$\Delta\phi_2=\frac{s_{11}m_{22}-s_{21}m_{12}}{s_{11}k_{22}-m_{12}^2}\Delta p_2. \tag{A1}$$

In addition, this pressure drop creates transverse effects: a pressure drop Δp_1 along the e_1 axis that induces recirculation, as well as a *transverse streaming current* $I_1=LJ_{el1}$ given by

$$\Delta p_1=-\frac{d}{L}\frac{s_{11}k_{12}-m_{11}m_{12}}{s_{11}k_{22}-m_{12}^2}\Delta p_2, \tag{A2}$$

$$I_1=LJ_{el1}=\frac{m_{12}}{s_{11}k_{22}-m_{12}^2}\Delta p_2. \tag{A3}$$

Electrically driven flow. In the case where no pressure drop exists between the two ends of the channel ($\Delta p_2=0$), effects may be generated by applying an electric current $J_{el2}\neq 0$ or an electric-field E_2 along e_2 (due to the short-circuited walls we have $J_1=0$, $\Delta\phi_1=0$). The applied field creates an electro-osmotic flow along the channel

$$J_2=\frac{M_{22}K_{11}-K_{21}M_{12}}{K_{11}}E_2 \tag{A4}$$

that is different from the case where the walls were not connected (see Sec. II B 2), if off-diagonal coefficients are nonzero. The electric conduction law is here $J_{el2}=[S_{22}K_{11}-M_{12}^2)/K_{11}]E_2$. *Transverse electro-osmosis* results in a pres-

sure difference $\Delta p_1 = d(M_{12}/K_{11})E_2$ and a total current intensity $I_1 = LJ_{el1} = L[(S_{12}K_{11} - M_{12}M_{11})/K_{11}]E_2$ through the connecting wires.

2. Continuous conducting electrodes

Due to the presence of the electrodes, any potential difference between the entrance and the exit of the channel is short circuited (i.e., a backward current runs along the electrodes in the e_2 direction) so that $\Delta\phi_2 = 0$ [Fig. 7(b)].

Pressure driven flow. A pressure drop along the channel ($\Delta p_2 \neq 0$) in this situation ($\Delta\phi_2 = 0$, $J_1 = 0$, $\Delta\phi_1 = 0$) again creates a transverse pressure drop across the channel Δp_1 synonymous of recirculation along the e_1 axis, as well as a *transverse streaming current* $I_1 = LJ_{el1}$ given by

$$\Delta p_1 = -\frac{d}{L}\frac{K_{12}}{K_{11}}\Delta p_2, \tag{A5}$$

$$I_1 = -\frac{M_{12}K_{11} - M_{11}K_{12}}{K_{11}}\Delta p_2. \tag{A6}$$

Transverse electro-osmotic pumping. But we may also consider the situation where an electric current J_{el1} is applied between the two walls. Formally, this case ($\Delta\phi_2 = 0$, $J_1 = 0$) allows electro-osmotic pumping in the e_2 direction, even in the absence of a driving pressure gradient in that direction ($\Delta p_2 = 0$). The resulting flow is

$$J_2 = \left(\frac{M_{21}K_{11} - K_{21}M_{11}}{K_{11}}\right)E_1 \tag{A7}$$

or $J_2 = [(M_{21}K_{11} - K_{21}M_{11})/(K_{11}S_{11} - M_{11}^2)]J_{el1}$. This is simply a manifestation of the transverse electro-osmosis mentioned in the first section of this section. It allows the design of lateral electro-osmotic pumps that do not require a global potential difference between the entrance and the exit of the channel (i.e., $\Delta\phi_2$ proportional to L) but rather local potential drops ($\Delta\phi_1$ proportional to d). For example, a potential difference $\Delta\phi_1$ of 1 V across a channel of width $d = 100$ μm, is enough to generate a transverse field $E_1 \sim 100$ V/cm, and thus pumping along the channel at $v_2 \sim 0.2$ mm/s.

APPENDIX B: SINUSOIDAL MODULATIONS OF SHAPE AND CHARGE DENSITIES

We propose here explicit formulas for the various components of the conductance and resistance matrices, obtained from the lubrication approximation in Sec. III, and summarized in Sec. III E, for the particular case of sinusoidal modulations of the height of the channel $h = h_0[1 + \alpha\cos(qx)]$ and of the charge densities $(\mu_1 + \mu_2)/2 = \mu_0 + \delta\mu\cos(qx + \Theta)$.

The lubrication approximation requires that $\alpha h_0 q \ll 1$. We here present explicit formulas that correspond to an expansion in α up to order α^2, assuming implicitly $\alpha \ll 1$. This provides a useful guide. The results are for the conductance matrix

$$K_x = \frac{h_0^3}{12\eta}(1 - 3\alpha^2), \quad K_y = \frac{h_0^3}{12\eta}\left(1 + \frac{3}{2}\alpha^2\right), \tag{B1}$$

$$S_x = \gamma_{el}h_0\left(1 - \frac{1}{2}\alpha^2\right), \quad S_y = \gamma_{el}h_0, \tag{B2}$$

$$M_x = -\mu_0 h_0\left[1 - \frac{3}{2}\alpha\frac{\delta\mu}{\mu_0}\cos(\Theta) - \frac{1}{2}\alpha^2\right], \tag{B3}$$

$$M_y = -\mu_0 h_0\left[1 + \frac{1}{2}\alpha\frac{\delta\mu}{\mu_0}\cos(\Theta)\right], \tag{B4}$$

and for the resistance matrix

$$k_x = \frac{12\eta}{h_0^3}(1 + 3\alpha^2), \quad k_y = \frac{12\eta}{h_0^3}\left(1 - \frac{3}{2}\alpha^2\right), \tag{B5}$$

$$s_x = \frac{1}{\gamma_{el}h_0}\left(1 + \frac{1}{2}\alpha^2\right), \quad s_y = \frac{1}{\gamma_{el}h_0}, \tag{B6}$$

$$m_x = \frac{12\eta\mu_0}{\gamma_{el}h_0^3}\left[1 - \frac{3}{2}\alpha\frac{\delta\mu}{\mu_0}\cos(\Theta) + 3\alpha^2\right], \tag{B7}$$

$$m_y = \frac{12\eta\mu_0}{\gamma_{el}h_0^3}\left[1 + \frac{1}{2}\alpha\frac{\delta\mu}{\mu_0}\cos(\Theta) - \frac{3}{2}\alpha^2\right]. \tag{B8}$$

Thus, for weak values of α, using Eq. (3) of Sec. II yields the ratios of transverse (F_{12}) to longitudinal (F_{11} or F_{22}) coefficients that typically appear in the formulas giving the effective overall transverse effects (see, e.g., Sec. II B and Appendix A):

$$k_{12}/k_{11} = k_{12}/k_{22} \simeq \frac{9}{2}\alpha^2\sin\theta\cos\theta, \tag{B9}$$

$$s_{12}/s_{11} = s_{12}/s_{22} \simeq \frac{1}{2}\alpha^2\sin\theta\cos\theta, \tag{B10}$$

$$m_{12}/m_{11} = m_{12}/m_{22} \simeq \left(-2\alpha\frac{\delta\mu}{\mu_0}\cos\Theta + \frac{9}{2}\alpha^2\right)\sin\theta\cos\theta, \tag{B11}$$

$$K_{12}/K_{11} = K_{12}/K_{22} \simeq -\frac{9}{2}\alpha^2\sin\theta\cos\theta, \tag{B12}$$

$$S_{12}/S_{11} = S_{12}/S_{22} \simeq -\frac{1}{2}\alpha^2\sin\theta\cos\theta, \tag{B13}$$

$$M_{12}/M_{11} = M_{12}/M_{22} \simeq \left(-2\alpha\frac{\delta\mu}{\mu_0}\cos\Theta - \frac{1}{2}\alpha^2\right)\sin\theta\cos\theta, \tag{B14}$$

where terms of order $\alpha^2(\delta\mu/\mu_0)^2$ have been omitted in the equations for m_{12} and M_{12}.

From these, three remarks may be made that substantiate the statements of Sec. III F.

(i) First, in the absence of a charge density modulation, all the effects are of order α^2.

(ii) Second, the prefactor of α^2 is purely geometrical, i.e., it does not involve an adimensional ratio of other physical quantities. Then remembering that the lubrication approximation solely requires $\alpha \ll 1/qh_0$, one is led to anticipate that in the case where $qh_0 \leqslant 1$, it is reasonable to expect that these ratio become of order one for a shape modulation comparable to the average gap thickness $\delta h/h \sim 1$.

(iii) If the average charge is almost zero so that $\delta\mu/\mu_0$ is very large, then in the limit $\alpha\delta\mu/\mu_0 \gg 1$, Eqs. (B11) and (B14) are to be replaced by purely geometrical ratios

$$m_{12}/m_{11} \simeq M_{12}/M_{11} \simeq \frac{4 \sin\theta \cos\theta}{3\cos^2\theta - \sin^2\theta}, \qquad \text{(B15)}$$

so that longitudinal effects may be totally dominated by transverse ones (see, e.g., Fig. 5), in particular in the vicinity of the ''magic angle'' $\theta = \pi/3$.

[1] *Micro Total Analysis Systems 2000*, edited by A. van den Berg, W. Olthuis, and P. Bergveld (Kluwer Academic Publishers, Dordrecht, 2000).

[2] A.D. Stroock and G. Whitesides, Phys. Today **54**, 42 (2001).

[3] G. Fuhr, T. Schnelle, and B. Wagner, J. Micromech. Microeng. **4**, 217 (1994).

[4] T. Müller *et al.*, Electrophoresis **14**, 764 (1993).

[5] M. Washizu, IEEE Trans. Ind. Appl. **34**, 732 (1998).

[6] B.S. Gallardo *et al.*, Science **283**, 57 (1999).

[7] D.J. Harrison *et al.*, Science **261**, 895 (1993).

[8] W. B. Russel, D. A. Saville, and W. R. Schowalter, *Colloidal Dispersions* (Cambridge University Press, Cambridge, 1989).

[9] A. Ajdari, Phys. Rev. Lett. **75**, 755 (1995); A. Ajdari, Phys. Rev. E **53**, 4996 (1996).

[10] J. Happel and H. Brenner, *Low Reynolds Number Hydrodynamics* (Martinus Nijhoff Publishers, The Hague, 1983).

[11] R. J. Hunter, *Foundations of Colloid Science* (Oxford University Press, New York, 1991).

[12] J.L. Anderson, Annu. Rev. Fluid Mech. **21**, 61 (1989).

[13] A.D. Stroock, *et al.*, Phys. Rev. Lett. **84**, 3314 (2000).

[14] S. L. Barker *et al.*, Anal. Chem. **72**, 4899 (2000).

[15] A. D. Stroock *et al.*, (unpublished).

[16] A. Ajdari, Phys. Rev. E **61**, R45 (2000).

[17] A.B.D. Brown, C.G. Smith, and A.R. Rennie, Phys. Rev. E **63**, 016305 (2001).